

# Structural and Optical Properties of Ce-Cupric Oxide Thin Films



Isam M.Ibrahim<sup>1</sup> , Jobair A.Najim<sup>2</sup>, Aws M.Rakea<sup>3</sup>

<sup>1</sup>Department of physics, College Science, University of Baghdad, Iraq

<sup>2</sup>Department of physics, College Science, University of Anbar, Iraq

<sup>3</sup>Department of physics, College Science, University of Anbar, Iraq

## ARTICLE INFO

Received: 5 / 2 /2017

Accepted: 17 / 4 /2017

Available online: 27/11/2018

DOI: [10.37652/juaps.2022.171601](https://doi.org/10.37652/juaps.2022.171601)

### Keywords:

Structural.

Optical Properties.

Thin Film.

CuO.

CeO.

## ABSTRACT

This work focuses discusses the structural and optical properties of Cerium- Cupric oxide thin film prepared on silicon and glass substrate by the spray pyrolysis technique at a temperature of 200,250,300 ° C. The results of (XRD) tests showed that all the prepared films were of a polycrystalline installation and monoclinic crystal structure with a preferable direction was (11 $\bar{1}$ ) of CuO. Morphology analysis studied by atomic force microscopy (AFM) and reveals that the grain size of the prepared thin film is approximately (64.69-101.26)nm , with a surface roughness of (0.238– 0.544) nm as well as root mean square of (0.280-0.636)nm for CuO Ce-doping, Optical characteristics were studied by UV/VIS Spectrophotometer at (300-1100 nm) and observed that the transmission value was more than 80 % at the visible wavelength range. The direct energy gap (E<sub>g</sub>) ranged between (1.70-3.00) eV at temperature 200 °C and then the values of the energy gap decreases with increasing temperature of substrate when, is measured by UV/VIS.

## 1. INTRODUCTION

The study and application of thin film technology is entirely entered in to almost all the branches of science and technology. Present study which describes the synthesis and study of optical, structural characteristics of cerium doped Cupric oxide (CuO) is really more interesting for researchers due to its vast applications[1].

Due to the properties like reflectivity, transparency, low electrical sheet resistance etc., copper oxide thin films has immense applications such as gas sensor devices[2] Solar application[3,4], magnetic devices[5], magnetic storage media[6], Optoelectronic Device[7], field emission[8].Till to day so many methods were adopted to synthesize doped or un-doped copper oxide films such as electrodeposition [9], spraying [10], CVD [11], thermal oxidation [12], MBE [13], plasma based ion

\* Corresponding author at: Department of physics, College Science, University of Baghdad, Iraq

.E-mail address:

implantation and deposition [14] and reactive sputtering Laser Pulse Evaporation, spray pyrolysis[15]. Cupric oxide crystallizes monoclinic structure with lattice constant 4.27 Å. It is an p-type semiconductor having low band gap energy ( $\approx 1.27$ -1.58 eV) [16,17] and the wavelength Cutting material (CuO) is (680) nm, either absorption coefficient is ( $10^4 \text{ cm}^{-1}$ ) when wavelength (500)nm ,Since Used in optical thermal complexes which require high efficiency and good range of stability and high absorbency in extent The visible wavelength[16,18]

## 2. EXPERIMENTAL

A Ce doped thin films at different concentration (10, 20,30,40 and 50 vol.%) of cerium ,were prepared by chemical spray pyrolysis. The films deposited onto silicon and micro-glass slides were first cleaned with detergent water and then dipped in Alcohol. Spray solution was prepared by mixing 0.1 M aqueous solutions of  $\text{CuCl}_2$  and  $\text{CeCl}_4$  at ratio (10, 20,30,40 and 50 vol.%) using a magnetic stirrer . The automated spray solution was then transferred to the hot substrate kept at the normalized deposition temperature of (200,250,and 300°C) using filtered air as carrier gas at a flow rate normalized to approximately(2.3) ml/min, to prevent the substrate from excessively cooling. The structural properties were determined by X-ray diffraction (XRD- 6000 Labx, supplied by Shimadzu, X-ray source is Cu). Film morphology was analyzed by atomic force microscope (AFM), type (CSPM).The optical absorption and transmission spectra were obtained using a UV-VIS spectrophotometer 6800JENWAY, Germany within the wavelength range of (300-1100) nm.

## 3. RESULTS AND DISCUSSION

### a. structural properties

The structure of the prepared Cupric oxide thin films were investigated by XRD. By observing the table 1 and Figure 1, which shows the test results x-Ray (XRD), And compare these Results with card (ASTM) (American Standard Testing of Materials) and the impact on silicon bases and thickness (175nm) found that The results are fairly compatible And by studying the diffraction pattern rays and see the peaks sites all films Prepared is undoped and doped cerium(10%), deposition on silicon substrate at 200°C, rules show that the films have Polycrystalline structure type Monoclinic the tendency has been for these films is (111) as well as the emergence of a second peak less intensity (11 $\bar{1}$ ), either the third peak was less stringent (20 $\bar{2}$ ) when Valuable tip diffraction angles all belong (CuO) When you increase the percentage of alcerium proportions, leaving (20, 30, 40, and 50) note increasing severity of peaks due to copper oxide as well as the emergence of new peaks to cerium oxide with decreased in (FWHM), with variation in offset angles, It turns out that increasing the temperature of deposited structure had not changed the nature of the Crystal structure of the article but has increased the intensity of the peaks as is evident in the figures 2 and 3 and tables 2 and 3. The result corresponds with that described by Motoyoshi, R et al [19].green size D was calculated using the diffraction results x-rays and it turns out that Crystal size increases with increasing doping with decreased (**FWHM**) these hard facts The existence of an inverse relationship between them.

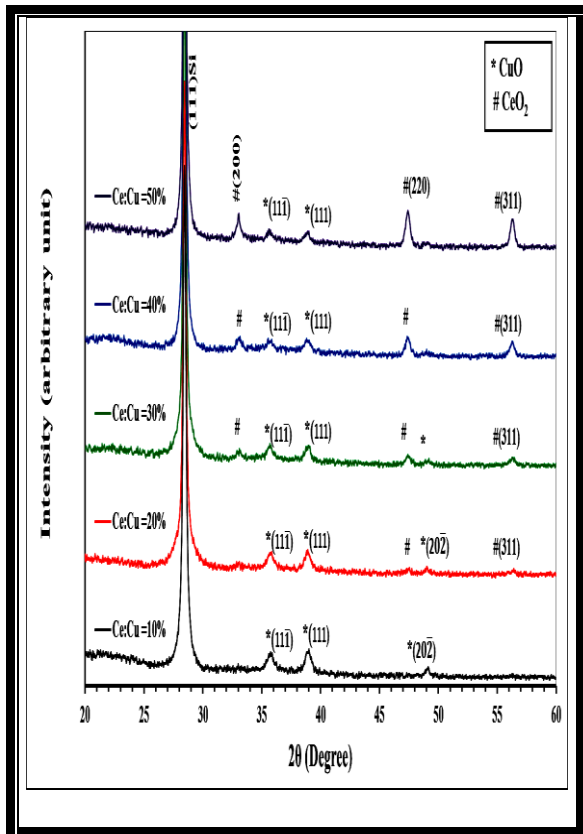


Figure1. X-ray diffraction patterns of Ce: CuO thin films at 200°C

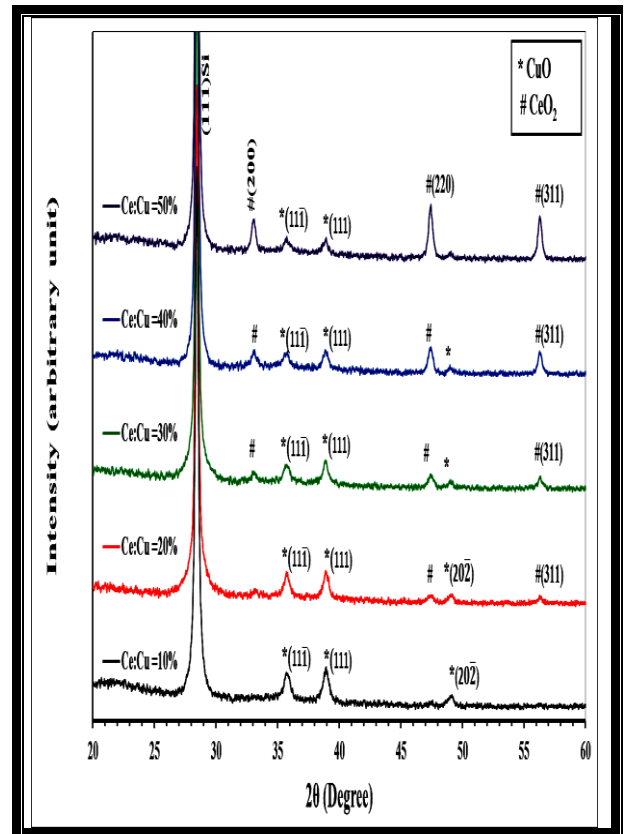


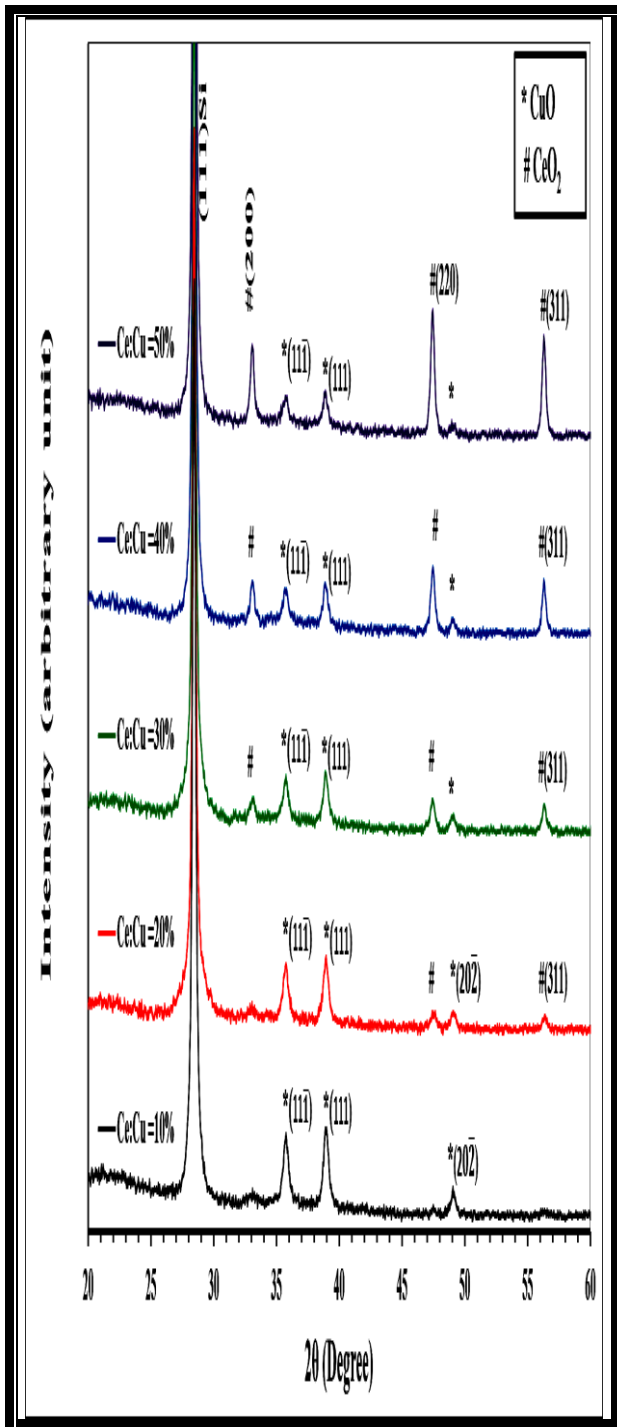
Figure2. X-ray diffraction patterns of Ce : CuO thin films at 250°C

Table 1: Average Crystallite size, d (hkl) and FWHM for Cerium - Cupric oxide thin films at 200°C

CeO <sub>2</sub> (%)	2θ (Deg.)	FWHM (Deg.)	d <sub>hkl</sub> Exp.(Å)	G.S (nm)	hkl	d <sub>hkl</sub> Std.(Å)	Phase	Card No.
10	35.7440	0.6340	2.5100	13.2	(11-1)	2.5108	CuO	96-900-8962
	38.9350	0.6000	2.3113	14.0	(111)	2.3118	CuO	96-900-8962
	49.0661	0.5600	1.8552	15.6	(20-2)	1.8553	CuO	96-900-8962
20	35.7316	0.6213	2.5108	13.4	(11-1)	2.5108	CuO	96-900-8962
	38.9226	0.5880	2.3120	14.3	(111)	2.3118	CuO	96-900-8962
	47.4390	0.5833	1.9149	14.9	(220)	1.9131	CeO <sub>2</sub>	96-900-9009
	49.0537	0.5488	1.8556	15.9	(20-2)	1.8553	CuO	96-900-8962
	56.3090	0.5560	1.6325	16.2	(311)	1.6315	CeO <sub>2</sub>	96-900-9009
30	33.0590	0.5068	2.7075	16.4	(200)	2.7055	CeO <sub>2</sub>	96-900-8962
	35.7192	0.6089	2.5117	13.7	(11-1)	2.5108	CuO	96-900-8962
	38.9102	0.5762	2.3127	14.6	(111)	2.3118	CuO	96-900-8962
	47.4280	0.5308	1.9154	16.4	(220)	1.9131	CeO <sub>2</sub>	96-900-9009
	49.0413	0.5378	1.8560	16.2	(20-2)	1.8553	CuO	96-900-8962
	56.2980	0.5060	1.6328	17.8	(311)	1.6315	CeO <sub>2</sub>	96-900-9009
40	33.0480	0.4612	2.7083	18.0	(200)	2.7055	CeO <sub>2</sub>	96-900-8962
	35.7068	0.5967	2.5125	14.0	(11-1)	2.5108	CuO	96-900-8962
	38.8978	0.5647	2.3134	14.9	(111)	2.3118	CuO	96-900-8962
	47.4170	0.4830	1.9158	18.0	(220)	1.9131	CeO <sub>2</sub>	96-900-9009
	56.2870	0.4604	1.6331	19.6	(311)	1.6315	CeO <sub>2</sub>	96-900-9009
50	33.0370	0.4197	2.7092	19.8	(200)	2.7055	CeO <sub>2</sub>	96-900-8962
	35.6944	0.5848	2.5134	14.3	(11-1)	2.5108	CuO	96-900-8962
	38.8854	0.5534	2.3142	15.2	(111)	2.3118	CuO	96-900-8962
	47.4060	0.4396	1.9162	19.7	(220)	1.9131	CeO <sub>2</sub>	96-900-9009
	56.2760	0.4190	1.6334	21.5	(311)	1.6315	CeO <sub>2</sub>	96-900-9009

Table 2: Average Crystallite size, d (hkl) and FWHM for Cerium - Cupric oxide thin films at 250°C

CeO <sub>2</sub> (%)	2θ (Deg.)	FWHM (Deg.)	d <sub>hkl</sub> Exp.(Å)	G.S (nm)	hkl	d <sub>hkl</sub> Std.(Å)	Phase	Card No.
10	35.7543	0.5706	2.5093	14.6	(11-1)	2.5108	CuO	96-900-8962
	38.9453	0.5400	2.3107	15.6	(111)	2.3118	CuO	96-900-8962
	49.0764	0.5040	1.8548	17.3	(20-2)	1.8553	CuO	96-900-8962
20	35.7419	0.5592	2.5101	14.9	(11-1)	2.5108	CuO	96-900-8962
	38.9329	0.5292	2.3114	15.9	(111)	2.3118	CuO	96-900-8962
	47.4603	0.5250	1.9141	16.5	(220)	1.9131	CeO <sub>2</sub>	96-900-9009
	49.0640	0.4939	1.8552	17.7	(20-2)	1.8553	CuO	96-900-8962
	56.3303	0.5004	1.6319	18.0	(311)	1.6315	CeO <sub>2</sub>	96-900-9009
30	33.0803	0.4561	2.7058	18.2	(200)	2.7055	CeO <sub>2</sub>	96-900-8962
	35.7295	0.5480	2.5110	15.2	(11-1)	2.5108	CuO	96-900-8962
	38.9205	0.5186	2.3122	16.3	(111)	2.3118	CuO	96-900-8962
	47.4493	0.4777	1.9145	18.2	(220)	1.9131	CeO <sub>2</sub>	96-900-9009
	49.0516	0.4840	1.8557	18.0	(20-2)	1.8553	CuO	96-900-8962
	56.3193	0.4554	1.6322	19.8	(311)	1.6315	CeO <sub>2</sub>	96-900-9009
40	33.0693	0.4151	2.7067	20.0	(200)	2.7055	CeO <sub>2</sub>	96-900-8962
	35.7171	0.5370	2.5118	15.5	(11-1)	2.5108	CuO	96-900-8962
	38.9081	0.5082	2.3129	16.6	(111)	2.3118	CuO	96-900-8962
	47.4383	0.4347	1.9150	20.0	(220)	1.9131	CeO <sub>2</sub>	96-900-9009
	49.0392	0.4744	1.8561	18.4	(20-2)	1.8553	CuO	96-900-8962
	56.3083	0.4144	1.6325	21.8	(311)	1.6315	CeO <sub>2</sub>	96-900-9009
50	33.0583	0.3777	2.7075	21.9	(200)	2.7055	CeO <sub>2</sub>	96-900-8962
	35.7047	0.5263	2.5127	15.9	(11-1)	2.5108	CuO	96-900-8962
	38.8957	0.4981	2.3136	16.9	(111)	2.3118	CuO	96-900-8962
	47.4273	0.3956	1.9154	21.9	(220)	1.9131	CeO <sub>2</sub>	96-900-9009
	56.2973	0.3771	1.6328	23.9	(311)	1.6315	CeO <sub>2</sub>	96-900-9009



**Figure3.** X-ray diffraction patterns of CuO: Ce thin films at 300°C

**Table 3:**Average Crystallite size,  $d_{hkl}$ ,  $hkl$  and FWHM for Cerium - Cupric oxide thin films at300°C

CeO <sub>2</sub> (%)	2θ (Deg.)	FWHM (Deg.)	$d_{hkl}$ Exp.(Å)	G.S (nm)	hkl	$d_{hkl}$ Std.(Å)	Phase	Card No.
10	35.7646	0.5135	2.5086	16.3	(11-1)	2.5108	CuO	96-900-8962
	38.9556	0.4860	2.3101	17.3	(111)	2.3118	CuO	96-900-8962
	49.0867	0.4536	1.8544	19.3	(20-2)	1.8553	CuO	96-900-8962
20	35.7522	0.5033	2.5095	16.6	(11-1)	2.5108	CuO	96-900-8962
	38.9432	0.4763	2.3109	17.7	(111)	2.3118	CuO	96-900-8962
	47.4706	0.4725	1.9137	18.4	(220)	1.9131	CeO <sub>2</sub>	96-900-9009
	49.0743	0.4445	1.8549	19.7	(20-2)	1.8553	CuO	96-900-8962
	56.3406	0.4504	1.6317	20.0	(311)	1.6315	CeO <sub>2</sub>	96-900-9009
30	33.0906	0.4105	2.7050	20.2	(200)	2.7055	CeO <sub>2</sub>	96-900-8962
	35.7398	0.4932	2.5103	16.9	(11-1)	2.5108	CuO	96-900-8962
	38.9308	0.4668	2.3116	18.1	(111)	2.3118	CuO	96-900-8962
	47.4596	0.4300	1.9142	20.2	(220)	1.9131	CeO <sub>2</sub>	96-900-9009
	49.0619	0.4356	1.8553	20.1	(20-2)	1.8553	CuO	96-900-8962
	56.3296	0.4098	1.6320	22.0	(311)	1.6315	CeO <sub>2</sub>	96-900-9009
40	33.0796	0.3736	2.7058	22.2	(200)	2.7055	CeO <sub>2</sub>	96-900-8962
	35.7274	0.4833	2.5111	17.3	(11-1)	2.5108	CuO	96-900-8962
	38.9184	0.4574	2.3123	18.4	(111)	2.3118	CuO	96-900-8962
	47.4486	0.3913	1.9146	22.2	(220)	1.9131	CeO <sub>2</sub>	96-900-9009
	49.0495	0.4269	1.8558	20.5	(20-2)	1.8553	CuO	96-900-8962
	56.3186	0.3729	1.6323	24.2	(311)	1.6315	CeO <sub>2</sub>	96-900-9009
50	33.0686	0.3399	2.7067	24.4	(200)	2.7055	CeO <sub>2</sub>	96-900-8962
	35.7150	0.4737	2.5120	17.6	(11-1)	2.5108	CuO	96-900-8962
	38.9060	0.4483	2.3130	18.8	(111)	2.3118	CuO	96-900-8962
	47.4376	0.3560	1.9150	24.4	(220)	1.9131	CeO <sub>2</sub>	96-900-9009
	49.0371	0.4184	1.8562	20.9	(20-2)	1.8553	CuO	96-900-8962
	56.3076	0.3394	1.6325	26.6	(311)	1.6315	CeO <sub>2</sub>	96-900-9009

Figure (4). As AFM examinations on film (Ce: CuO rates % (10, 20,30,40, and 50 %) It shows the presence of homogenous grains throughout the film and shows the distribution of particles on the surface of the film and two the first two dimensions (2D) and second in three dimensions (3D) and we observed that average surface roughness and average root men square (RMS) value increasing with increasing of Ce%, as shown in table 4 and explain that a Crystal development for grained vertically on the surface.

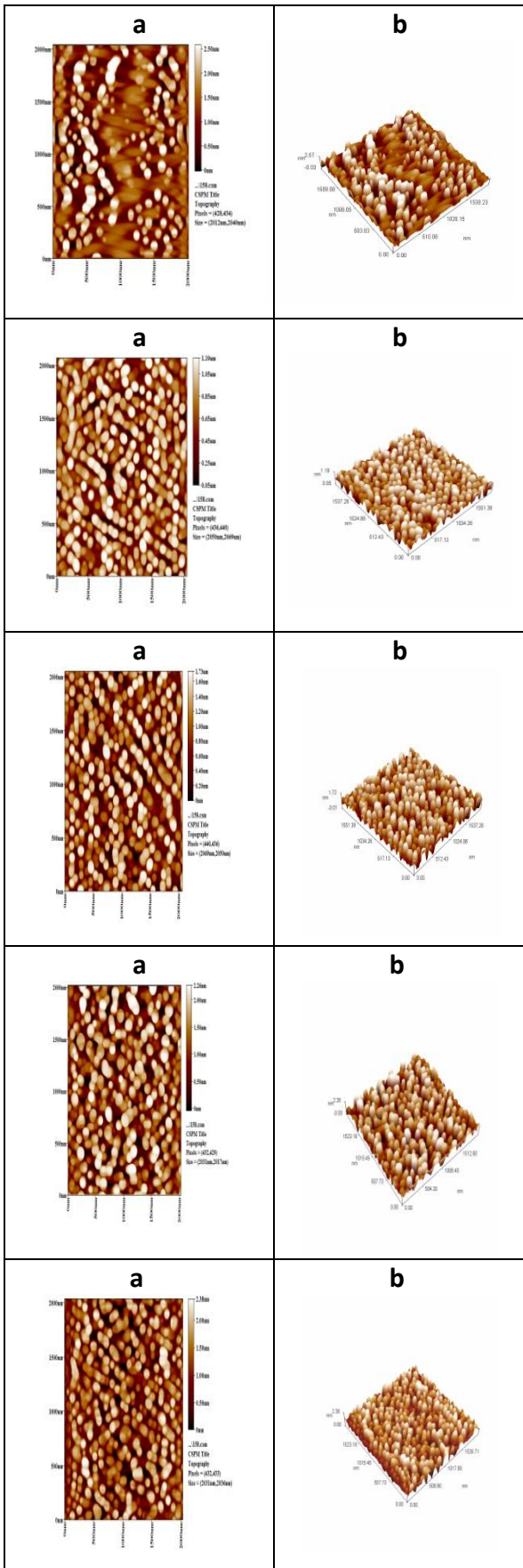


**Figure4** The atomic force microscope (a) 2-D and (b) 3-D Image of prepared films

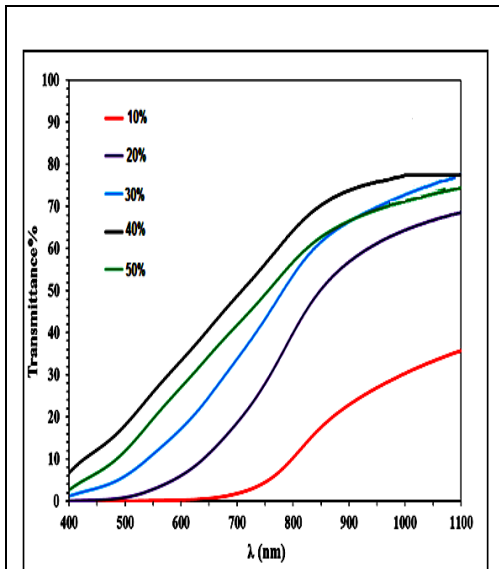
**Table 4:** The Average grain sizes, roughness average and(RMS) for CeO<sub>2</sub> - CuO films

%CeO <sub>2</sub>	Average diameter (nm)	Roughness (nm)	(r.m.s.) nm
10	64.69	0.238	0.280
20	73.63	0.388	0.452
30	76.61	0.496	0.512
40	85.49	0.500	0.590
50	101.26	0.544	0.636

**b. Optical properties:**

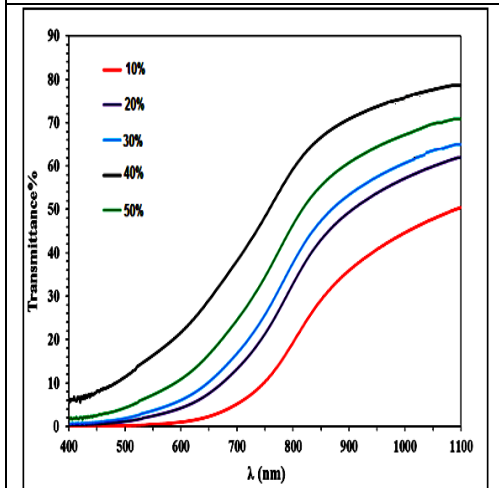
The transmittance is measured when wavelength (300-1100)nm and notice of Form (5) the transmittance increases progressively with increasing wavelength, as doped films in proportions gravimetric (10, 20,30,40, and 50%) start at the lowest value when the wavelength (400nm) then look almost constant within the range length wavelength (600-800nm) to rise rapidly to wavelength (800-1100 nm) and explained that this Opaque materials behave articles (opaque materials) and a window for the IR (infrared), as we observed that increasing transmittance of films prepared with increasing cerium doped as shift toward the low energy (red shift) It turns out that increasing the temperature of deposited substrate rules leads to decrease transmittance and all ratios, as shown in Figure 5. The experimental result agrees with that reported by Sekhar C and Ogwu, A. et al [20, 21]. And we noticed that absorbcency behave "differently" transmittance taking absorption spectrum exponential decay with increasing wavelength due to low energy photons and inability to raise electrons from the valence band to conductive band , an inverse relationship between wavelength and energy of photon [22].





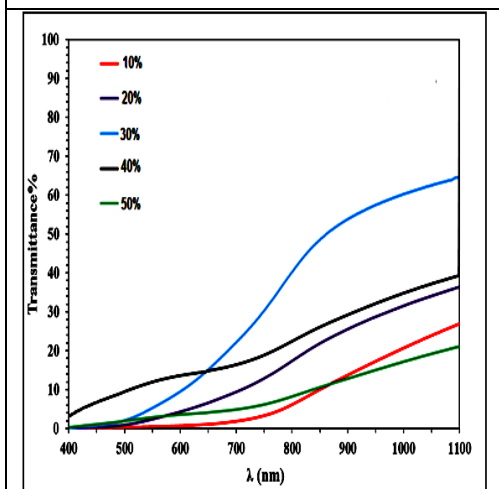
(a)

Figure 5-a The transmittance of prepared films



(b)

Figure 5-b The transmittance of prepared film



(c)

Figure 5-c The transmittance of prepared films

**Figure 6-** The current study found, one type of basic electronic transitions and electronic transitions Allowable direct, through which the optical energy gap values were calculated for films prepared so optical energy gap values were calculated for Allowable direct transition for all copper oxide films [20,21].

$$(\alpha h\nu)^2 = \beta(h\nu - E_g) \quad \text{-----(2)}$$

Where  $\alpha$  is the absorption coefficient,  $\beta$  is a constant,  $E_g$  is the optical energy gap,  $\nu$  is the incident photon frequency, and his Planck.

The graphical relationship between  $(\alpha h\nu)^2$  as a function of photon energy ( $h\nu$ ) and that tangent line the straight part of the curve represents the value of the optical energy gap of the allowed direct transition, most researchers depend on this way calculate the energy gap likes (Balamurugan et al ) [22], as well as researchers Papadimitropoulos et al [23], for Cupric oxide films with Ce (10,20, 30,40, 5%), Energy gap values gradually increased with increasing proportions of cerium This means that doping caused by the resulting offset edge absorption toward high energies that's when the degree of the base 200°C. The heat when the temperature increases at 250,300 °C, the increased energy gap less than the values. Table-5 shows the energy gap for all films prepared values.

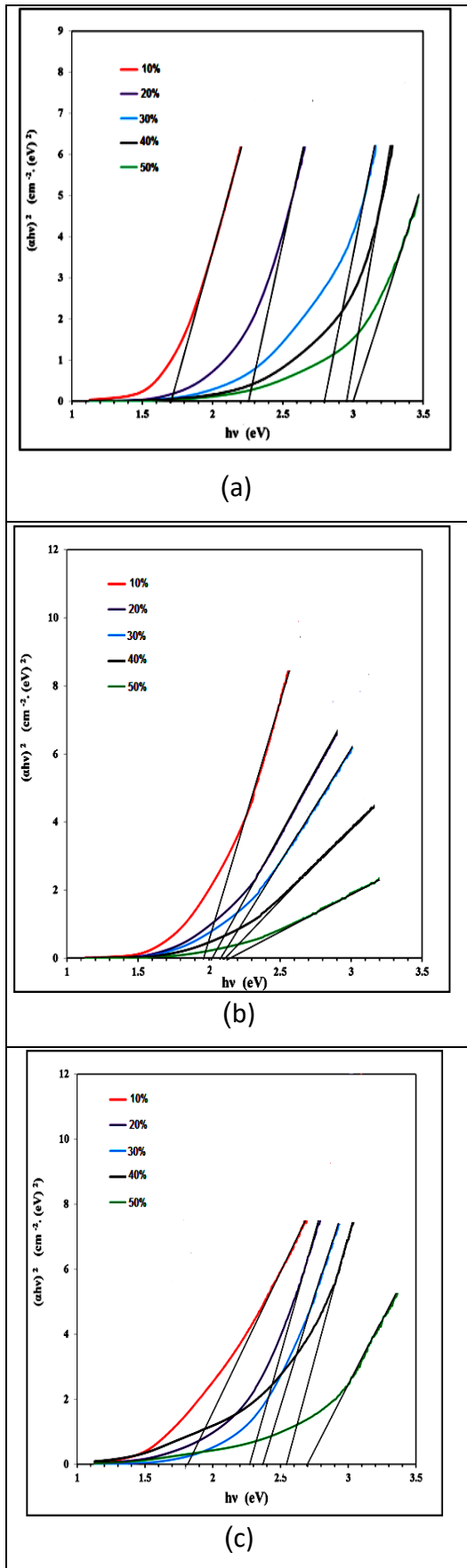


Figure 6. Band gap for CuO-CeO<sub>2</sub> films at different temperature a)200°C, b)250°C and c) 300°C

Table 5: Band gap energies calculated with Tauc method

Ce%	Eg (eV)at 200°C	Eg (eV)at 250°C	Eg (eV)at 300°C
10%	1.70	1.95	1.80
20%	2.25	2.05	2.20
30%	2.80	2.08	2.37
40%	2.95	2.12	2.55
50%	3.00	2.15	2.70

### Conclusion

All the films have Polycrystalline structure type Monoclinic the tendency has been for these films is (111) at temperatures substrate (200, 250and 300 °C ), Adding cerium did not change the nature of the crystal structure, adding led to a increase in crystal size ( $D$ ) with decreasing width mid-intensity ( $FWHM$ ) as illustrated by the results X ray, the beloved structures within structures of nanoparticles, this is illustrated by the results of X-rays. Surface roughness average and the root mean square (RMS) increasing their values when adding for all films and increasing rate grain size as indicated by (AFM), films transmittance increases and absorbance decreases with increasing ratios of Ce%, and that the energy gap increases with increasing cerium ratios.

### REFERENCES

- [1] Chen BJ, Sun XW, Tay BK. Fabrication of ITO thin films by filtered cathodic vacuum arc deposition. Mater. Sci. Eng. B., 106: 300-304, (2004).
- [2] El Amrani A, Hijazi F, Lucas B, Bouclé J, Aldissi M. Electronic transport and optical properties of thin oxide films. Thin Solid Films, 518: 4582- 4585, (2010).

- [3] X.P. Gao, J.L. Bao, G.L. Pan, H.Y. Zhu, P.X. Huang, F. Wu, D.Y. Song, "Preparation and Electrochemical Performance of Polycrystalline and Single Crystalline CuO Nanorods as Anode Materials for Li Ion Battery", *J. Phys. Chem.*, Vol. 108, PP. 5547, (2004).
- [4] H.M. Xiao, S.Y. Fu, L.P. Zhu, Y.Q. Li, G. Yang, Eur, "Controlled synthesis and characterization of CuO nanostructures through a facile hydrothermal route in the presence of sodium citrate", *J. Inorg. Chem.*, Vol. 14, (2007).
- [5] H. Fan, L. Yang, W. Hua, X. Wu, Z. Wu, S. Xie, B. Zou, "Controlled synthesis of monodispersed CuO nanocrystals", *Nanotechnology Nanotechnology*, Vol. 15, P. 37, (2008).
- [6] C.T. Hsieh, J.M. Chen, H.H. Lin, H.C. Shih, "Field emission from various CuO nanostructures", *Applied Physics Letters*, Vol. 83, P. 3383, (2003).
- [7] P.O. Larsson, A. Andersson, R.L. Wallengerg, B. Svensson, "Catalytic Oxidation of 1,2-Dichlorobenzene over Supported Transition Metal Oxides", *J. Catal.*, Vol. 163, P. 279, (1996)
- [8] W. Chae, J. Ho Yoon, H. Yu, D. Jang, Y. Kim, "Ultraviolet Emission of ZnS Nanoparticles Confined within a Functionalized Mesoporous Host", *J. Phys. Chem.*, Vol. 108, P. 11509, (2004)
- [9] Y. Liu, Y. Liu, R. Mu, H. Yang, C. Shao, J. Zhang, Y. Lu, D. Shen, and X. Fan, "The structural and optical properties of Cu<sub>2</sub>O films electrodeposited on different substrates," *Semicond. Sci. Technol.*, 20, 44, (2005).
- [10] Y. C. Zhou and J. A. Switzer, "Galvanostatic electrodeposition and microstructure of copper(I) oxide film," *Mater. Res. Innovat.*, 2, 22, (1998).
- [11] T. Maruyama, "Copper oxide thin films prepared from copper dipivaloylmethanete and oxygen by chemical vapor deposition," *Jpn. J. Appl. Phys.*, 37, 4099, (2000).
- [12] V. Figueiredo, E. Elangovan, G. Gonçalves, P. Barquinha, L. Pereira, N. Franco, E. Alves, R. Martins, and E. Fortunato, "Effect of post-annealing on the properties of copper oxide thin films obtained from the oxidation of evaporated metallic copper," *Applied Surface Science*, 254, 3949, 2008.
- [13] R. Kita, K. Kawaguchi, T. Hase, T. Koga, R. Itti, and T. Morishita, "Effect of oxygen ion energy on the growth of CuO films by molecular beam epitaxy using mass-separated low energy O<sup>+</sup> beams," *J. Mater. Res.*, 9, 1280, (1994).
- [14] Xinxin Ma, Gang Wang, Ken Yukimura, and Mingren Sun, "Characteristics of copper oxide films deposited by PBII&D," *Surface and Coatings Technology*, 201, 6712, (2007).
- [15] F. Drobny and D. Pulfrey, "Properties of reactively sputtered copper oxide thin films," *Thin Solid Films*, 502(1/2): 205–211, (2006).
- [16] F. Bayansal, B. Sahin, M. Yuksel, H.A. Cetinkara "SILAR- based growth of



- nanostructured CuO thin films from alkaline baths containing saccharin as additive" J. Materials Letters Vol. 98 Pages: 197-200 Provider: Elsevier,( 2013).
- [17] M Izaki, "Effects of annealing on optical and electrical characteristics of p- type semiconductor copper (II) oxide electrodeposits " Journal: Thin Solid Films Vol. 520 ,P. 2434-42437 Provider: Elsevier, (2012).
- [18]Z.H. Gan, G.Q. Yu, B.K. Tay, C.M. Tan, Z.W. Zhao, Y.Q. Fu," Preparation and characterization of copper oxide thin films deposited by filtered cathodic vacuum arc" J..Appl. Phys, Vol. 37, P. 81, (2004).
- [19] Motoyoshi, R., Oku, T., Kidowaki, H., Suzuki, A., Kikuchi, K., Kikuchi, S. & Jeyadevan, B.. "Structure and photovoltaic activity of cupric oxide-based thin film solar cells". Journal of the Ceramic Society of Japan 118(1383): 1021-1023,(2010).
- [20] Sekhar C.,Ray." Praration of copper oxide thin film by sol-gel-like dip technique and study of their structure and optical properties. Journal of physics. Slar energy materials and solar cells 68:307-312 (2001).
- [21] Ogwu, A.A. Bouquerel, E., Ademosu, O., Moh, S., Crossan ,E, and Placido, F. An investigation of the surface energy and optical transmittance of copper oxide thin .lms prepared by reactive magnetron sputtering Thin Film Centre, Electronic Engineering and Physics Division,.,Acta Materialia 53 :5151–5159,(2005).
- [22] مؤيد جبرائيل" فيزياء الحالة الصلبة"مديرية دار الكتب للطباعة والنشر/الموصل,ج, 1 الاولى (1987).
- [23] M. S. Dresselhaus , "Optical Properties of Solids" Part II , (1998).
- [24] Y. Liu, Y. Liu, R. Mu, H. Yang, C. Shao, J. Zhang, Y. Lu, D. Shen, and X. Fan, "The structural and optical properties of Cu<sub>2</sub>O films electrodeposited on different substrates," Semicond. Sci. Technol., 20, 44, (2005).
- [25] Balamurugan ,B. and Mehta, B.R..Optical and structural properties of nanocrystalline Copper Oxide thin films prepared by activated reactive evaporation, Thin Solid Films 396: 90-96,(2001).
- [26] Papadimitropoulos ,G., N. Vourdas, N., Vamvakas, E., Davazoglou ,D.. "Optical and structural properties of copper oxide thin films grown byoxidation of metal layers Institute of Microelectronics". Thin Solid Films 515 :2428–2432,(2006).

## الخصائص التركيبية والبصرية لأغشية أكسيد السيريوم-النحاس الرقيقة

عصام محمد ابراهيم<sup>1</sup> ، جبير عبدالله نجم<sup>2</sup> ، أوس موفق راع<sup>3</sup>

<sup>1</sup>قسم الفيزياء- كلية العلوم، جامعة بغداد- العراق  
<sup>2</sup>قسم الفيزياء- كلية العلوم، جامعة الأنبار- العراق  
<sup>3</sup>قسم الفيزياء- كلية العلوم، جامعة الانبار- العراق

### الخلاصة:

تم في هذا البحث مناقشة الخصائص التركيبية والبصرية لأغشية أكسيد السيريوم-أكسيد النحاس الرقيقة المرسبة على قواعد من السيليكون والزجاج بواسطة تقنية التحلل الكيميائي الحراري في درجات حرارة مختلفة °C 200، 300، 250، وأظهرت نتائج حيود الأشعة السينية (XRD) أن جميع الأغشية المحضرة تمتلك تركيب متعدد التبلور (polycrystalline) أحادية الميل (monoclinic) وان الاتجاه المفضل هو (11<sup>-1</sup>). درست طوبوغرافية السطح من خلال مجهر القوة الذرية (AFM) وقد تبين أن الحجم الحبيبي للأغشية الرقيقة المحضرة حوالي (64.69-101.26)nm، مع خشونة السطح (0.238- 0.544) nm وكذلك متوسط الجذر التربيعي (RMS) (0.280-0.636)nm لأغشية أكسيد النحاس- سيريوم الرقيقة المحضرة، وقد تمت دراسة الخصائص البصرية بواسطة مطياف النفاذية للأشعة المرئية - فوق البنفسجية (UV-VIS) عند طول موجي (300 - 1100 nm)، ولوحظ أن قيمة النفاذية كانت أكثر من 80% في نطاق الطول الموجي المرئي وان فجوة الطاقة المباشرة تمتلك قيم متدرجة بين (1.70-3.00) eV عند درجة حرارة °C 200، ثم تتخفف قيم فجوة الطاقة مع زيادة درجة حرارة القاعدة.